

# GCN-MPPR: Enhancing the Propagation of Message Passing Neural Networks via Motif-Based Personalized PageRank

Mingcan Wang

mingcan\_wl@163.com

School of Computer Science and  
Engineering, Northeastern University  
Shenyang, Liaoning, China

Xian Zhang

School of Computer Science and  
Engineering, Northeastern University  
Shenyang, Liaoning, China

Junchang Xin\*

xinjunchang@mail.neu.edu.cn

School of Computer Science and  
Engineering, Northeastern University  
Key Laboratory of Big Data  
Management and Analytics (Liaoning  
Province), Northeastern University  
Shenyang, Liaoning, China

Kaifu Long

School of Computer Science and  
Engineering, Northeastern University  
Shenyang, Liaoning, China

Zhongming Yao

zyao@cs.aau.dk

The Department of Computer Science,  
Aalborg University  
Aalborg, Danmark

Zhiqiong Wang

wangzq@bmie.neu.edu.cn

College of Medicine and Biological  
Information Engineering,  
Northeastern University  
Shenyang, Liaoning, China

## Abstract

The algorithms based on message passing neural networks (MPNNs) on graphs have recently achieved great success for various graph applications. However, studies find that these methods always propagate the information to very limited neighborhoods with shallow depth, particularly due to over-smoothing. That means most of the existing MPNNs fail to be so ‘deep’. Although some previous work tended to handle this challenge via optimization- or structure-level remedies, the overall performance of GCNs still suffers from limited accuracy, poor stability, and unaffordable computational cost. Moreover, neglect of higher-order relationships during the propagation of MPNNs has further limited the performance of them.

To overcome these challenges, a novel variant of PageRank named motif-based personalized PageRank (MPPR) is proposed to measure the influence of one node to another on the basis of considering higher-order motif relationships. Secondly, the MPPR is utilized to the message passing process of GCNs, thereby guiding the message passing process at a relatively ‘high’ level. The experimental results show that the proposed method outperforms almost all of the baselines on accuracy, stability, and time consumption. Additionally, the proposed method can be considered as a component that can underpin almost all GCN tasks, with DGCRN being demonstrated in the experiment. The **anonymous** code repository is available at: <https://anonymous.4open.science/r/GCN-MPPR-AFD6/>.

## CCS Concepts

- Computing methodologies → Knowledge representation and reasoning; Neural networks; Machine learning algorithms; • Information systems → Web mining; Social networks.

## Keywords

Graph Neural Network, Network Motif, Motif-Based Personalized PageRank, Propagation, Message Passing Neural Network.

### ACM Reference Format:

Mingcan Wang, Junchang Xin\*, Zhongming Yao, Xian Zhang, Kaifu Long, and Zhiqiong Wang. 2026. GCN-MPPR: Enhancing the Propagation of Message Passing Neural Networks via Motif-Based Personalized PageRank. In *Proceedings of The 2026 SIGKDD Conference (Conference acronym 'XX)*. ACM, New York, NY, USA, 11 pages. <https://doi.org/XXX>

## 1 Introduction

Graph is a ubiquitous structure that garners significant interest from both academic and industrial communities [1–5]. Effective mining on graphs will benefit a wide range of applications, such as web advertising [6] and social network analysis [7]. The deep learning methods have achieved remarkable successes in different analysis levels of node, link and graph, which cannot be neglected in any possible manner. There are many approaches for conducting deep learning algorithms on graphs. Early methods such as node embedding techniques [8, 9] typically rely on random walks or matrix factorization to learn node representations directly, often in an unsupervised fashion and without incorporating node features. In contrast, many modern approaches jointly leverage both graph structure and node features within a supervised (or semi-supervised) framework. Representative examples include spectral graph convolutional neural networks [10–12], message passing (neighbor aggregation) algorithms [13–15], and neighbor aggregation methods based on recurrent neural networks [16–18].

Among these methods, message passing neural networks (MPNNs) have received particularly intense attention in recent years for its

Permission to make digital or hard copies of all or part of this work for personal or classroom use is granted without fee provided that copies are not made or distributed for profit or commercial advantage and that copies bear this notice and the full citation on the first page. Copyrights for components of this work owned by others than the author(s) must be honored. Abstracting with credit is permitted. To copy otherwise, or republish, to post on servers or to redistribute to lists, requires prior specific permission and/or a fee. Request permissions from [permissions@acm.org](mailto:permissions@acm.org).

Conference acronym 'XX, Jeju, Korea

© 2026 Copyright held by the owner/author(s). Publication rights licensed to ACM.

ACM ISBN XXX-X-XXXX-XXXX-X/2026/04

<https://doi.org/XXX>

flexibility and good performance. The past few years have seen significant advances in enhancing the message passing mechanism, including attention-based approaches [19, 20], stochastic process integrations [21, 22], and so on. Despite these impressive developments, the robustness and scalability of message passing algorithms remain frequently questioned. In MPNNs, sufficient layers of propagation are necessary to capture more information of nodes within the network, as deeper architectures allow aggregation of multi-hop neighborhood information and thus model longer-range dependencies more effectively. However, aggregation through averaging often results in highly similar learned features, a phenomenon widely known as over-smoothing. As a result, existing message-passing neural networks are typically constrained by shallow-layer information, limiting their ability to fully exploit the rich structural patterns in large or complex graphs.

Recent study [23] proposed to combine personalized PageRank (PPR) with the message passing neural network, and came up with a novel framework that emphasizes ‘predict and propagate’ to solve the problem. Since PPR uses the idea of random walk, the proposed method can propagate the information more deeply without adding layers with the aid of PPR. And their work has broadened the development of the message passing algorithms [24, 25]. However, all of these methods are about MPNNs plus a linear model (e.g. PPR), neglecting the higher-order relationships. This prevents the proposed method from capturing the higher-order relationships and guiding the propagation based on them. Consequently, the current propagations of MPNNs are still restricted by limited shallow information. And the following challenges faced by existing works restricts the performance of MPNNs.

**Challenge I: Depth-induced homophily collapse.** Despite ongoing efforts to mitigate over-smoothing through techniques like structure-level [26, 27] or optimization-level [28–30] remedies, the over-smoothing problem has not been completely resolved. Shallow-layer propagation would result in shallow information of nodes, while simply enlarging the number of layers in MPNNs cannot effectively enable the model to acquire more discriminative information and may even result in homophily collapse. As a result, developing more effective propagation methods remains one of the major challenges.

**Challenge II: Failure to utilize higher-order relationships.** In the predominant frameworks of MPNNs as well as many variants of them such as VGAE[31] and PPNP [23], the vast majority of models rely heavily on linear transformations and linear gradient descent throughout their message-passing and updating steps (e.g., linear aggregations and linear projections). This linearity-centric design dominates the methods and largely overlooks the prevalence of higher-order relational structures – such as motifs – that are ubiquitous in real-world networks and play a crucial role in network science. Consequently, conventional MPNNs struggle to capture rich, non-pairwise dependencies and multi-way interactions, limiting their expressive power on heterophilic, hierarchical, or combinatorially complex graphs.

**Challenge III: Trade-offs in accuracy, stability, and computational efficiency.** In MPNNs, accuracy, stability, and computational efficiency are all critically important; a significant compromise in any one of these dimensions will directly impair the model’s predictive performance, training reliability, and real-world

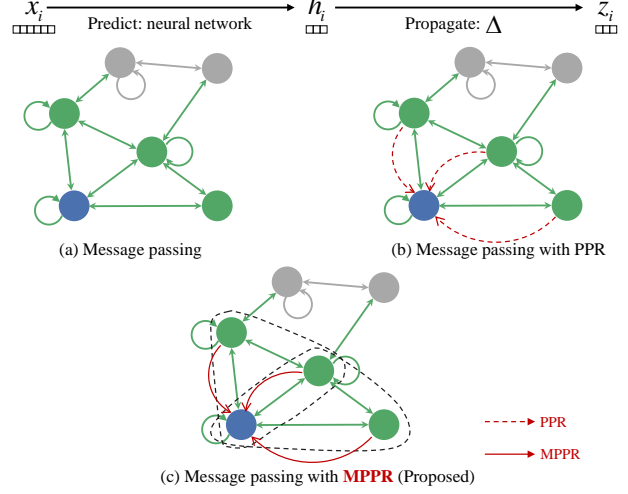


**Figure 1: Visualization of the contributions of GCN-MPPR upon existing works, whereas  $\Delta$  = (a) message passing; (b) message passing with PPR and (c) message passing with MPPR (spreading information further considering higher-order motifs).**

scalability. Existing remedies—whether structure-level modifications or optimization techniques—often improve one aspect at the expense of others, leading to unstable training, high computational overhead, or marginal accuracy gains across tasks like node classification and link prediction. Then how to modify the MPNN models to ensure an overall improvement is another challenge.

To alleviate the problems mentioned above, firstly, a novel network metric named motif-based personalized PageRank (MPPR) is proposed to measure and reflect the influence of one node to another on the basis of considering higher-order motif relationships. Secondly, the MPPR is utilized to the message passing process of GCNs, yielding a novel framework named GCN-MPPR, which tends to guide the propagation of message passing process based on MPPR. This would allow enlarging the covering domain of specific nodes without adding the layers of GCNs and causing over-smoothing. The differences between GCN-MPPR and existing work are visualized in Figure 1. Theoretically, since MPPR emphasizes the higher-order relationships in the graphs, message passing via MPPR can guide the training process more accurately and efficiently on the basis of considering higher-order motif relationships, thus upgrading the accuracy, stability and computational efficiency. Experimentally, it is demonstrated that GCN-MPPR is competitive among the baselines in both node classification and link prediction tasks. Furthermore, experiments also verify the GCN-MPPR can be easily integrated into many state-of-the-art methods as a component and upgrade the performance. To summarize, the contributions of this work can be summarized as:

- Proposing MPPR, a novel network metrics to measure the influence of one node to another based on PageRank and motif, that can inherit the expressive power of motifs to effectively capture complex, higher-order relationships beyond traditional pairwise interactions.

- Applying MPPR to the propagation of MPNNs, which enables a more accurate and effective message aggregation process in different tasks of graphs, enabling the models to be more faithful for higher-order relational patterns without incurring prohibitive computational overhead.
- Conducting thorough experiments, demonstrating that the proposed method not only achieves competitive performance against competitors across various tasks, but also serves as a plug-and-play component that consistently improves performance when integrated into MPNN models.

The rest of the paper is organized as follows. Related work is reviewed in section 2. Section 3 defines the problem and the proposed methods. The proposed method and the competitors are evaluated in section 4. Finally, section 5 concludes the paper. Relative appendixes appear in Appendix.

## 2 Related Work

### 2.1 Network Motif

Motif, also known as graphlets or subgraphs, characterizes higher-order relations in complex networks, which was first introduced in [32]. Rather than consider the linear relationship within each network only, motif can capture the multi-node interactions in the topological structure. For example, in social networks, the existence of the ‘triangular motif’ ( $A \leftrightarrow B, A \leftrightarrow C, B \leftrightarrow C$ ) can enhance the cohesion of the group. The influence of  $A$  on  $B$  is indirectly amplified through  $C$  (the interaction between  $B$  and  $C$  is jointly influenced by  $A$ ), which is a common nonlinear relationship. Then the edge existing in more triangular motifs is considered more important than the one existing in less or none triangular motifs. Also in web graphs, the more motifs a link is evolved, the more important the link should be considered. Therefore, the capacity of capturing nonlinear relationships makes motifs useful in many applications, such as web networks, social networks, neuroscience networks and bioinformatics networks.

As most of the previous work focused on how to efficiently count the number of motifs in complex networks [33–36], it was proven that motifs can be used for graph/web mining tasks [37, 38]. For instance, Zhao *et al.* [39] proposed to rank the users in social networks via motif-based PageRank, which enhances the ranking ability of PageRank by capturing higher-order relationships using motif and incorporating them into PageRank. Wu *et al.* [40] introduced a motif-based contrastive graph clustering approach with clustering oriented prompt, which employs a specialized Siamese encoder network to obtain both lower-order and higher-order node embeddings. The encoder processes both views of the graph: one based on lower-order adjacency and the other on higher-order motif structures, and the higher-order motif (such as triangles) is extracted using motif adjacency matrices.

### 2.2 PageRank and Personalized PageRank

Apart from ranking web pages as its original aim, PageRank (PR) [41] has been used in domains as vast as web graph analysis, resource allocation and so on. For example, Zhao *et al.* [39] proposed to rank the social network users via motif-based PageRank, a variant of PageRank that emphasize higher-order relationships. Zhao *et al.* [42] proposed to rank the Chinese medicine acupoints by

introducing higher-order interactions between multiple acupoints and PageRank in the acupoint-disease network. As a variant of the PageRank, Personalized PageRank (PPR) is designed to measure the importance of nodes in a graph with respect to a specific ‘personalization’ node (or set of nodes). In PageRank, each node’s score is a weighted sum of the scores of its neighbors, with a small probability of teleporting to a specific node in the graph. Comparatively, PPR modifies this by restricting teleportation to a specific set of personalization node(s), thus biasing the scores toward nodes that are close to these personalization node(s) in the graph. This makes it more than popular in many applications, such as recommendation systems [43, 44].

### 2.3 MPNN Meets Personalized PageRank

In order to alleviate the over-smoothing problem of normal MPNNs, Gasteiger *et al.* [23] proposed to use the relationship between graph convolutional networks (GCN) and PageRank to derive an improved propagation scheme based on personalized PageRank, namely PPNP. And they proposed a approximate version of it, named approximate PPNP (APPNP). Inspired by this, Bojchevski *et al.* [24] proposed to scale GNN upon networks with millions of nodes by utilizing an efficient approximation of information diffusion, resulting in significant speed gains while maintaining relatively state-of-the-art prediction performance. Li *et al.* [25] built the theoretical link between the temporal message passing scheme adopted by T-GNNs and the temporal random walk process on dynamic graphs, which indicates that it would be possible to select a few influential temporal neighbors to compute a target node’s representation without compromising the predictive performance. They then proposed to utilize T-PPR, a parameterized metric for estimating the influence score of nodes on evolving graphs. Ma *et al.* [45] proposed personalized PageRank graph neural network for TF-target gene interaction detection method, namely PPRTGI.

### 2.4 Main Contributions against Related Works

Compared to the previous works, first and foremost, Motif-Based Personalized PageRank (MPPR) is proposed, a latest variant of PPR or PR. MPPR can rank the importance between a pair of nodes on the basis of considering the high-order motifs of the network structure, thereby being more receivable and comprehensive. Secondly, inspired by PPNP [23], MPPR is applied to the message passing process of graph convolutional networks, yielding GCN-MPPR, enabling the information of nodes to spread farther and faster without enlarging the number of layers and causing over-smoothing, thus improving the accuracy and computational efficiency of GCN models. Finally, the proposed MPPR can be regarded as a component, which can play an active role in speeding up and improving the accuracy in many MPNN architectures, with DGCRL being verified as an example in this paper.

## 3 Graph Neural Networks with Motif-Based Personalized PageRank

In this section, we first introduce the notations and definitions of the paper. Second, the details of MPPR is discussed, which is a latest variant of PPR. Then, the GCN-MPPR framework for both node classification and link prediction is detailed.

### 3.1 Notations and Preliminaries

Let  $G = (V, E)$  be an unweighted directed graph, where  $V = \{v_1, \dots, v_n\}$  is node set with cardinality  $|V| = n$  and  $E = \{e_1, \dots, e_m\}$  is edge set with cardinality  $|E| = m$ . The features of nodes are denoted as  $X \in \mathbb{R}^{n \times f}$ , with the number of features notated as  $f$  for each node. And the labels (or classes) are denoted as  $Y \in \{0, 1\}^{n \times C}$  with the number of classes denoted as  $C$ . The graph  $G$  is described by the adjacency matrix  $A \in \mathbb{R}^{n \times n}$ , while  $\tilde{A} = A + I_n$  denotes the adjacency matrix with added self-loops. Denote  $\tilde{A}' = \tilde{D}^{-1/2} \tilde{A} \tilde{D}^{-1/2}$  as the symmetrically normalized adjacency matrix with self-loops, whereas  $\tilde{D}_{ij} = \sum_k \tilde{A}_{ik} \delta_{ij}$  is the diagonal degree matrix. Given the above notations, the PageRank value vector  $\psi$  of the nodes can be calculated by iteration as,

$$\psi_t = d \cdot \mathbf{P}^T \psi_{t-1} + \frac{1-d}{n} \mathbf{e} \quad (1)$$

where  $d \in (0, 1]$  is the damping factor,  $t$  is the iteration time,  $\mathbf{e} \in \mathbb{R}^n$  is a vector with each element equal to 1 and  $\mathbf{P}$  is obtained by  $\mathbf{P} = A_{ij} / \sum_j A_{ij}$ . And the calculation process has been proved to be converged [46]. As the concept of personalized PageRank defines the root node  $v_i$  via the teleport vector  $i_{v_i}$ , a one-hot indicator vector, the adaptation of personalized PageRank can be obtained for node  $x$  using:  $\pi_{\text{ppr}}(v_i) = (1 - \alpha) \cdot \tilde{A}' \cdot \pi_{\text{ppr}}(v_i) + \alpha \cdot i_{v_i}$ , with the teleport (or restart) possibility  $\alpha \in (0, 1]$ . By solving the equation, we obtain  $\pi_{\text{ppr}}(v_i) = \alpha \cdot \left( I_n - (1 - \alpha) \tilde{A}' \right)^{-1} i_{v_i}$ . Since  $i_{v_i}$  is a vector containing only one '1' value at the corresponding position except '0', which allows us to preserve the node's local neighborhood even in the limit distribution, it is possible to union  $\pi_{\text{ppr}}(v_1), \dots, \pi_{\text{ppr}}(v_n)$ , yielding the full personalized PageRank matrix:

$$\Pi_{\text{ppr}} = \alpha \cdot \left( I_n - (1 - \alpha) \tilde{A}' \right)^{-1} \quad (2)$$

For the ease of description of the following contents, the definitions of motif and motif set is borrowed from [39, 47] and presented.

**Definition 3.1.** Motif. A motif  $M$  is defined on  $k$  nodes by a tuple  $(B, \mathcal{A})$ , where  $B$  is a  $k \times k$  binary matrix, and  $\mathcal{A} \in \{1, 2, \dots, k\}$  specifies the anchor set, which is the set of the indices of the anchor nodes.

In **Definition 3.1**, a graph encoding the edge patterns between the  $k$  nodes are represented by  $B$  and a subset of the  $k$  nodes for defining the motif-based adjacency matrix is denoted as  $\mathcal{A}$ . To put it differently, two nodes will be regarded as occurring in a given motif only when their indices belong to  $\mathcal{A}$ . As usual, anchor nodes are all of the  $k$  nodes, in which case the motif is called simple motif; Otherwise, it is called anchored motif. In this work, we only consider the case of simple motif, and more specifically three-node simple motif. Given the definition above, we can define the set of motif as follows.

**Definition 3.2.** Motif set. A motif set, notated as  $\mathcal{M}(B, \mathcal{A})$ , in an unweighted directed graph  $G$  with adjacency matrix  $A$  is defined as:

$$\mathcal{M}(B, \mathcal{A})$$

$$= \{(\text{set}(v), \text{set}(\chi_{\mathcal{A}}(v))) \mid v \in V^k, v_1, \dots, v_k, \text{distinct}, A_v = B\} \quad (3)$$

where  $\mathbf{v}$  is an ordered vector representing the indices of  $k$  nodes, and  $A_v$  is the  $k \times k$  adjacency matrix of the subgraph induced by  $\mathbf{v}$ .  $\chi_{\mathcal{A}}(\cdot)$  is a selection function that takes the subset of a  $k$ -tuple indexed by  $\mathcal{A}$ , and  $\text{set}(\cdot)$  is an operator that transforms an ordered tuple to an unordered set, thus  $\text{set}((v_1, v_2, \dots, v_k)) = \{v_1, v_2, \dots, v_k\}$ .

### 3.2 Motif-Based Personalized PageRank

Given an unweighted graph  $G$ , the PageRank (PR) value represents the importance of each node, and the personalized PageRank (PPR) measures the importance range of each pair. From Equation 1 and Equation 2, it is obtained that adjacency matrix  $A$  can affect both  $\mathbf{P}$  and  $\tilde{A}'$ , thus the final PR or PPR values. However, for both PR and PPR, the values are calculated based on the direct pair-wise relations, neglecting the higher-order relationships. To solve this problem, the concept of PageRank is combined with motif and yield motif-based personalized PageRank (MPPR). Motif can be regarded as a pattern of edges on a small number of nodes from a graph that can capture higher-order information in the network. PPR is a metric that can measure the importance of different nodes in the network. Thus, they can complement with each other, and the proposed MPPR is a metric that reflects the importance of different nodes in the network in consideration of the higher-order motifs. Note all of the motifs concerned in this paper refers to network motifs, rather than biology motifs. The following of this subsection introduces the calculation of MPPR.

Following [39, 47], given a motif set  $\mathcal{M}(B, \mathcal{A})$ , the motif-based adjacency matrix or co-occurrence matrix of a type of motif  $M_i$  is defined as:

$$A_{ij}^{M_i} = \sum_{(v, \chi_{\mathcal{A}}(v)) \in M_i} \mathbb{1}(\{i, j\} \subset \chi_{\mathcal{A}}(v), i \neq j) \quad (4)$$

where  $\mathbb{1}(St) = 1$  if the boolean variable  $St$  is *True* and otherwise 0. The motif-based adjacency matrix  $A^{M_i}$  represents the frequency of two nodes appearing in a given motif. The higher  $A_{ij}^{M_i}$  is, the more significant the relation between  $i$  and  $j$  is within the network in consideration of motif  $M_i$ . In this work, only three-node motifs are considered. And among the three-node motifs, we further restrict our focus on seven kinds of triangular motifs (Figure 2a) since the importance of them in networks has been verified by many studies [48, 49]. The computation results of motif-based adjacency matrices for  $M_1$  to  $M_7$  in Figure 2(a) is grabbed from [39, 47], which are presented in Appendix A.

Take Figure 2(b) as an example, the normal adjacency matrix of the network is given as (i), and motif-based adjacency matrix of  $M_7$  motif is described as (ii). The corresponding values of  $v_1 \rightarrow v_3$  and  $v_3 \rightarrow v_1$  are both 2, because the edges  $v_3 \rightarrow v_1$  exists in two  $M_7$ -based motifs ( $\langle v_1, v_3, v_4 \rangle; \langle v_1, v_2, v_3 \rangle$ ). The motif-based adjacency matrix is always symmetric. This is because it emphasizes how many motifs is an edge involved, rather than the dependence relationship of the linked nodes. In this paper, it is argued that the edge-based and motif-based relationships complement each other in measuring the relationships among the nodes. Thus, a simple yet effective linear transformation is applied to combine the edge-based and motif-based adjacency matrices:

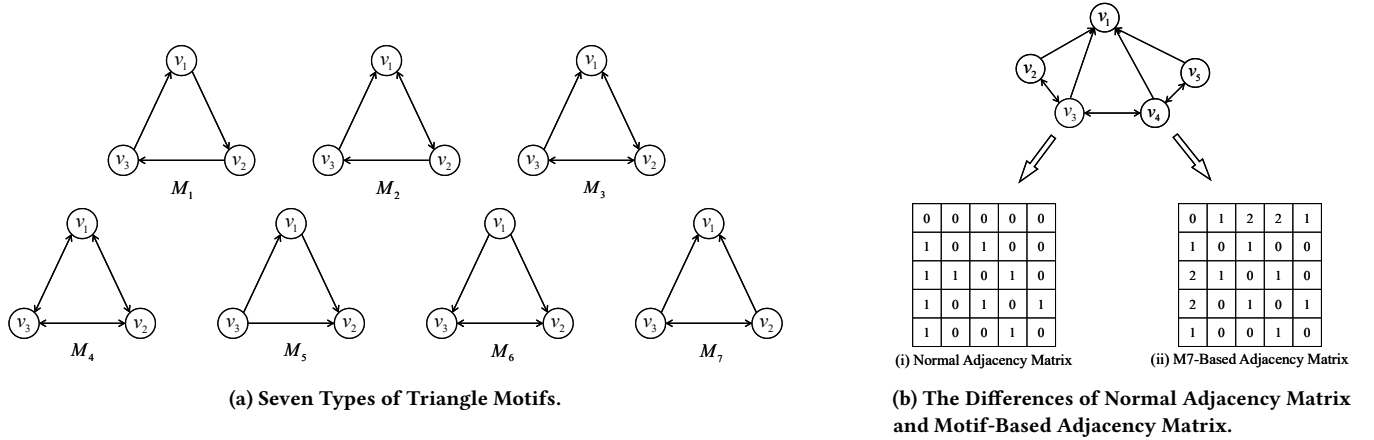


**Figure 2: Visualization of Seven Types of Motifs Considered and the Example for the Calculation of Motif-Based Adjacency Matrix.**

$$\mathbf{A}^{M_k} = (1 - \tau) \mathbf{A} + \tau \mathbf{A}^{M_k} \quad (5)$$

where  $\tau \in [0, 1]$  balances the edge-based and motif-based relations,  $\mathbf{A}$  is the original adjacency matrix and  $\mathbf{A}^{M_k}$  is the calculated motif-based adjacency matrix. By removing the  $\tilde{\mathbf{A}}$ ' in Equation 2 by  $\mathbf{A}^{M_k}$ , the MPPR is calculated as,

$$\Pi_{\text{MPPR}} = \alpha \cdot \left( \mathbf{I}_n - (1 - \alpha) \mathbf{A}^{M_k} \right)^{-1} \quad (6)$$

which reflects the importance among nodes on the basis of considering higher-order motif relationships within the networks.

### 3.3 GCN-MPPR for Node Classification

Then, we consider a simple and widely used message passing algorithm for semi-supervised classification, graph convolutional network (GCN). In the case of two-layer message passing, the equation can be formulized as:

$$Z_{\text{GCN}} = \text{softmax} \left( \tilde{\mathbf{A}}' \text{ReLU} \left( \tilde{\mathbf{A}}' \mathbf{X} \mathbf{W}_0 \right) \mathbf{W}_1 \right) \quad (7)$$

where  $Z_{\text{GCN}} \in \mathbb{R}^{n \times c}$  is the predicted labels,  $\tilde{\mathbf{A}}'$  is discussed above and  $\mathbf{W}_1$  and  $\mathbf{W}_2$  are the trained weights. In such two-layer GCNs, only neighbors within the two-hop neighborhood are covered. This means that these neural networks fail to be so 'deep'. In this work, MPPR is combined with MPNNs, which guides the propagation process at a 'higher-order' level, resulting in a better and more promising propagation scheme.

In order to utilize the preceding higher-order relationships for semi-supervised classification, predictions for each node are generated based on its own features and then they are propagated via MPPR introduced above to generate the final predictions. In such a way, the GCN-MPPR is founded, which results in changing Equation 7 to:

$$\begin{aligned} Z_{\text{MPPR}} &= \left( \alpha \cdot \left( \mathbf{I}_n - (1 - \alpha) \mathbf{A}^{M_k} \right)^{-1} \right)^\beta \mathbf{H} \\ H &= f_\theta(X), \quad H \in \mathbb{R}^{|V| \times C}. \end{aligned} \quad (8)$$

where  $\mathbf{X}$  is the feature matrix and  $f_\theta$  is a neural network with parameter set  $\theta$ ,  $\mathbf{H} \in \mathbb{R}^{n \times c}$  is the generated predictions and  $\beta$  is defined as a slipping factor.

The final class probabilities are obtained by applying a row-wise softmax,

$$P = \text{softmax}(Z). \quad (9)$$

Only a small subset of nodes  $\mathcal{V}_{\text{train}} \subset V$  is labeled during training. The model is trained end-to-end by minimizing the cross-entropy loss over labeled nodes:

$$\mathcal{L}_{\text{node}} = - \sum_{v \in \mathcal{V}_{\text{train}}} \sum_{c=1}^C Y_{vc} \log P_{vc}. \quad (10)$$

Gradients are backpropagated through both the neural network  $f_\theta$  and the propagation operator, enabling the model to implicitly leverage information from large graph neighborhoods while avoiding oversmoothing.

Similar to PPNP [23], GCN-MPPR separates the neural network used for generating predictions from the propagation scheme. This separation thus solves the second problem discussed in section 1. The depth of the neural network is now fully independent of the propagation algorithm. It is important to note that GCN-MPPR is also trained end-to-end. That is, the gradient flows through the propagation scheme during backpropagation (implicitly considering infinitely many neighborhood aggregation layers). Compared to PPNP, however, the proposed GCN-MPPR solves the propagation issue by motif-based personalized PageRank, which considers the higher-order relationships of nodes in the considered network. Adding the propagation effects based on MPPR significantly upgrades the model's performance.

### 3.4 GCN-MPPR for Link Prediction

Then, we introduce the GCN-MPPR framework for link prediction. We stick to the upmentioned notations and definitions to study link prediction based on GCN-MPPR.  $\mathbf{X} \in \mathbb{R}^{|V| \times d}$ . To avoid information leakage, we first split observed edges into training/validation/test sets. All message passing and propagation are performed on the training graph  $G_{\text{train}} = (V, E_{\text{train}})$ , which is obtained by removing

the validation and test positive edges from  $E$ . For supervision, we pair each mini-batch of positive edges with an equal number of negative samples (non-edges) and optimize a binary classification objective.

Our encoder follows the Personalized PageRank Neural Network (PPNP) principle by decoupling feature transformation from graph propagation. Specifically, we compute local node representations with a two-layer multilayer perceptron (MLP)  $f_\theta$  with ReLU activations and dropout:

$$H = f_\theta(X). \quad (11)$$

We then diffuse these representations over  $G_{\text{train}}$  using a motif-based personalized pageRank operator with teleport (restart) probability  $\alpha \in (0, 1)$ . Let  $\tilde{A}$  denote the (symmetrically) normalized adjacency matrix of  $G_{\text{train}}$ . The PPR propagation can be written in closed form as

$$Z = \Pi_{\text{MPPR}} H = \left( \alpha \cdot \left( I_n - (1 - \alpha) \mathbf{9}^{M_k} \right)^{-1} \right)^\beta H, \quad (12)$$

Given the final node embeddings  $Z$ , we score a candidate edge  $(u, v)$  using a dot-product decoder, which is then mapped into an existence probability with the activation function (logistic sigmoid as an example in this paper):

$$p_{uv} = \sigma(z_u^\top z_v) = \frac{1}{1 + \exp(-s_{uv})}. \quad (13)$$

The model is trained end-to-end with binary cross-entropy on positive edges and negative samples:

$$\mathcal{L} = - \sum_{(u,v) \in \mathcal{E}^+} \log p_{uv} - \sum_{(u,v) \in \mathcal{E}^-} \log(1 - p_{uv}), \quad (14)$$

where  $\mathcal{E}^+$  and  $\mathcal{E}^-$  denote the sets of positive and negative training pairs, respectively.

## 4 Experimental Results and Analysis

In this section, comparative evaluations of GCN-MPPR against baselines are first performed on well-designed semi-supervised node classification and link prediction tasks. Then, GCN-MPPR is applied in a latest GCN-related framework named DGCRL to estimate how much GCN-MPPR would benefit for it.

### 4.1 Datasets and Baselines

Four datasets are applied for node classification and link prediction tasks, namely Cora [50], PubMed [51], Amazon computers and Amazon photo [52]. The details of these datasets are presented in Appendix B. Basic models including GCN [53] and GAT [54] are selected as baselines for both tasks. For node classification, the baselines also contain GIN [55], PPNP (& APPNP) [23], PPRGo [24], SHP-GNN [56]. For link prediction, GAE (& VGAE) [31] and HDGL [57] are considered for evaluation.

### 4.2 Node Classification Results

In order to verify the advantages of GCN-MPPR, we first utilize a well-designed semi-supervised node classification task to test the performance of it with its competitors.

**4.2.1 Experimental Settings.** In the experiments, each dataset is divided into a visible training set and an invisible test set, which do not change. The test set was only used once to report the final performance. Additionally, the *early stopping* criterion the same as PPNP and APPNP is applied across models, whose details can be referred to [23]. To maintain fairness, the neural network for GCN-MPPR is structurally very similar to GCN and PPNP and has the same number of parameters. Two layers with  $h = 64$  hidden units are used. To avoid overfitting, we apply  $L_2$ -regularization with  $\lambda = 0.005$  on the weights of the first layer and use dropout with dropout rate  $d = 0.5$  on both layers and the adjacency matrix. For the teleport probability of MPPR,  $\alpha = 0.1$ . The slipping factor  $\beta$  for *Cora* and *Pubmed* is set as 0.5, and 0.75 for the other datasets. The parameter  $\tau$  applied in Equation 5 is set as 0.9. Each experiment is conducted 100 times on multiple random splits. The average and variance of accuracy are reported.

**4.2.2 Classification Accuracy Results.** The classification accuracy of various models is presented in Table 1. The results of GCN-MPPR are presented in bold if it outperforms all of the baselines. First, it is obvious that almost all of the classification accuracy of GCN-MPPR is higher than all of the baselines, no matter which type of motif structure is considered (from  $M_1$  to  $M_7$ ). Second, the performance of GCN-MPPR on PubMed network is not so competitive. This could be partly attributed to the fact that the motif within this network is less meaningful, which even poses a negative effect of the classification accuracy on GCN-MPPR. However, even in this case, the gap between GCN-MPPR and the best performer on PubMed network is quite narrow. Meanwhile, the training process of GCN-MPPR saves more than 60% time than many the baselines (further discussed in subsubsection 4.2.3). Furthermore, the variance of GCN-MPPR is significantly lower than the competitors. This means that the addition of MPPR on GCN improves the stability of traditional GCN models. As a consequence, there are enough evidences to believe in the performance of GCN-MPPR. The box plots of 100-run experiments on various datasets are presented in Appendix C, which further demonstrate the stability of GCN-MPPR.

**4.2.3 Classification Runtime Results.** The runtime analysis is conducted on Amazon Computers network, and results are shown in Table 2. The best performer on runtime is shown in bold, and the second-best performer is presented underlined. It could be seen that GCN-MPPR is much faster than all of the baselines except PPRGo on the total time and the training time per epoch. This is because, with the addition of MPPR, it can accelerate the propagation process greatly by propagating the information deeper and more proper. In this way, the *early stopping* condition is achieved faster. It is important to emphasize that the approximate PPNP saves a lot of time during the calculation of PPR than PPNP, rather than saves the time during training. Thus, it is reasonable to find that its training time is even longer than PPNP, since Table 2 considers the runtime comparison only. Though PPRGo is fast than GCN-MPPR, its performance is yet limited as is presented in Table 1 and mentioned above. This shows that PPRGo is extremely competitive when scaling MPNNs to networks with millions of nodes, rather than making accurate classifications, which agrees with the birth of PPRGo. As for the training time per epoch, GCN-MPPR, PPNP and APPNP are about slower than GCN, which is mainly because of the larger number of

**Table 1: The Accuracy Results of Node Classification via GCN-MPPR and its competitors.**

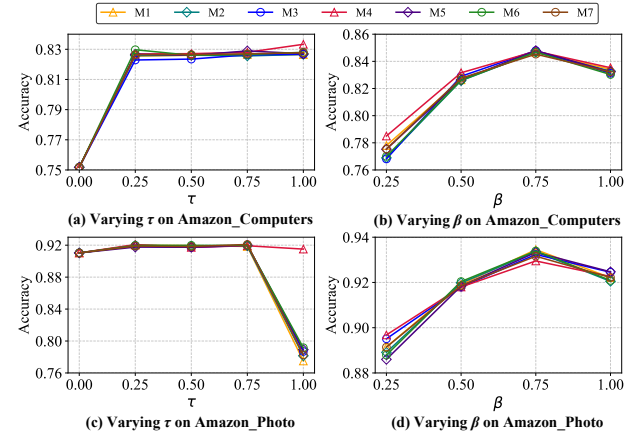
	Cora	PubMed	Amazon_computers	Amazon_photo
GCN	$0.7836 \pm 0.0195$	$0.7765 \pm 0.4000$	$0.7422 \pm 0.2350$	$0.9023 \pm 0.1088$
GAT	$0.7908 \pm 0.0105$	$0.7776 \pm 0.4400$	$0.7662 \pm 0.5615$	$0.8942 \pm 0.2062$
GIN	$0.7605 \pm 0.0805$	$0.7695 \pm 0.3301$	$0.7588 \pm 0.8142$	$0.8901 \pm 0.4468$
PPNP	$0.8247 \pm 0.0118$	$0.8021 \pm 0.0172$	$0.7722 \pm 0.1400$	$0.9113 \pm 0.0649$
APPNP	$0.8234 \pm 0.0121$	$0.8009 \pm 0.0173$	$0.7664 \pm 0.1518$	$0.9121 \pm 0.0618$
PPRGo	$0.8201 \pm 0.2563$	$0.7148 \pm 0.1151$	$0.6528 \pm 0.5540$	$0.6990 \pm 0.6532$
SHP-GNN	$0.7721 \pm 0.0325$	<b><math>0.8058 \pm 0.0725</math></b>	$0.7656 \pm 0.0725$	$0.9008 \pm 0.0332$
GCN-MPPR <sub>M1</sub>	<b><math>0.8276 \pm 0.0123</math></b>	$0.7935 \pm 0.0138$	<b><math>0.8467 \pm 0.0137</math></b>	<b><math>0.9345 \pm 0.0061</math></b>
GCN-MPPR <sub>M2</sub>	<b><math>0.8253 \pm 0.0131</math></b>	$0.7940 \pm 0.0126$	<b><math>0.8468 \pm 0.0139</math></b>	<b><math>0.9336 \pm 0.0066</math></b>
GCN-MPPR <sub>M3</sub>	<b><math>0.8265 \pm 0.0096</math></b>	$0.7941 \pm 0.0125$	<b><math>0.8479 \pm 0.0126</math></b>	<b><math>0.9324 \pm 0.0058</math></b>
GCN-MPPR <sub>M4</sub>	$0.8163 \pm 0.0106$	$0.7938 \pm 0.0176$	<b><math>0.8475 \pm 0.0126</math></b>	<b><math>0.9295 \pm 0.0056</math></b>
GCN-MPPR <sub>M5</sub>	<b><math>0.8273 \pm 0.0109</math></b>	$0.7938 \pm 0.0124$	<b><math>0.8479 \pm 0.0132</math></b>	<b><math>0.9333 \pm 0.0059</math></b>
GCN-MPPR <sub>M6</sub>	<b><math>0.8302 \pm 0.0106</math></b>	$0.7937 \pm 0.0130$	<b><math>0.8468 \pm 0.0130</math></b>	<b><math>0.9339 \pm 0.0066</math></b>
GCN-MPPR <sub>M7</sub>	<b><math>0.8334 \pm 0.0089</math></b>	$0.7942 \pm 0.0125$	<b><math>0.8453 \pm 0.0140</math></b>	<b><math>0.9316 \pm 0.0066</math></b>
GCN-MPPR <sub>Mean</sub>	<b><math>0.8266</math></b>	$0.7939$	<b><math>0.8470</math></b>	<b><math>0.9326</math></b>

**Table 2: Time Consumption Analysis During Propagation on Amazon Computers Network.**

	Total Time	Last Epoch	Average Per Epoch
GCN	102.18s	3050	33.50ms
GAT	178.81s	1980	90.26ms
PPNP	75.85s	1715	44.22ms
APPNP	96.91s	2069	46.88ms
PPRGo	<b>6.59s</b>	200	<b>32.95ms</b>
SHC-Concat	59.71s	820	72.80ms
GCN-MPPR	<b>29.10s</b>	860	<b>33.83ms</b>

matrix multiplications. Meanwhile, the training time per epoch of GCN-MPPR is less than the ones of PPNP and APPNP. This could be partially attributed to the fact that the calculated MPPR is sparser than PPR, thereby reducing the time of matrix multiplications. It is worth emphasizing that GCN-MPPR is faster than other models such as PPNP mainly because it can lead the training process wiser and more proper due to the higher-order motif consideration, such that the *early stopping* condition is achieved faster.

**4.2.4 Hyper-Parameter Analysis.** For the model, this work has three hyper-parameters,  $\tau$ ,  $\alpha$ , and  $\beta$ . Since the reasonable selection of  $\alpha$  has already been fully discussed in related references for PageRank [25, 41, 58], we do not discuss it in this article. We conduct experiments regarding the setting of  $\tau$  and  $\beta$  respectively to test the parameter sensitivity of the model on *Amazon\_computers* dataset. First, we set  $\tau \in [0, 0.25, 0.5, 0.75, 1]$ . Noticeably, when  $\tau = 0$ , the GCN-MPPR degenerates into PPNP, and when  $\tau = 0$  the linear relationships in Equation 5 is totally neglected. As shown in the Figure 3(a) and 3(c), compared to  $\tau = 0$  or  $\tau = 1$ , the performance of GCN-MPPR is significantly better, which demonstrates that the complementary effect of Equation 5 and utilization of MPPR is effective. Meanwhile, it shows that GCN-MPPR is almost robust throughout different settings of  $\tau$  except  $\tau = 0$  or  $\tau = 1$ . Then, as is shown in Figure 3(b) and 3(d), when  $\beta$  rises from 0.25 to 0.75, the performance of GCN-MPPR increases, though the increase rate drops a little after  $\beta$  reaches 0.5. After that, the performance of GCN-MPPR drops a little as  $\beta$  increases from 0.75 to 1. This is mainly

**Figure 3: Accuracy when varying parameters.**

because that the calculated MPPR matrix is relatively sparse. Thus, we need  $\beta$ -power ( $\beta < 0$ ) to enlarge and activate some elements in the matrix. However, the setting of  $\beta$  should not be too little yet. According to the hyper-parameter analysis, we observe the ideal setting of  $\beta$  should range from 0.5 to 0.75.

**4.2.5 Ablation Study.** The ablation study is carried out in both ways on *Amazon Computers* Network. One the one hand, we remove the motif and MPPR on GCN-MPPR respectively. One the other hand, as the MPPR propagation scheme affecting (a) the neural network during training, and (b) the classification decision during predicting, it is worthwhile to investigate how the model performs without propagation during (a), (b) or both of them. Table 3 shows whether MPPR is effective and whether the MPPR-based propagation affects both training and predicting. First, the optimal results come from the full propagation of GCN-MPPR, which validates our approach. And the performance of propagation during prediction only is quite satisfactory for both PPNP and GCN-MPPR. This re-verifies the conclusion in [23] that these models can be combined with pre-trained models that do not incorporate any

**Table 3: The Results of Ablation Study.**

	None	Train	Predict	Train & Predict	
w/o MPPR		69.0%			
w/o Motif (PPNP)	69.0%	71.5%	75.8%	77.2%	
GCN-MPPR <sub>Mean</sub>	69.0%	71.5%	76.3%	82.6%	

graph information and still significantly improve their accuracy. It also shows that just propagating during training can also result in improvements. This indicates that GCN-MPPR can also be applied to online/inductive learning where only the features and not the neighborhood information of an incoming (previously unobserved) node is available.

### 4.3 Link Prediction Results

**4.3.1 Experimental Settings.** In case of link prediction experiments, all datasets are firstly preprocessed by selecting the largest connected component and removing self-loops. Node features are used in their original bag-of-words or attribute form without additional normalization or dimensionality reduction. Positive edge samples are directly taken from the undirected edges present in each graph. We adopt a transductive random edge splitting protocol. For each independent run, train/validation/test = 5:1:4; To ensure the training graph remains connected, we first extract a BFS spanning tree and force all its edges into the training set. The remaining edges are then randomly allocated to validation, test, or training sets. Negative samples are generated at a 1:1 ratio (one negative per positive edge). All negatives are sampled from the full original graph to avoid including any true existing edges. For GCN, PPNP and GCN-MPPR, we adopt classic 2-layer GCNs, using a hidden dimension of 64 and an output embedding dimension of 64. Training is performed with the Adam optimizer (learning rate 1e-3 in all experiments). The maximum number of training epochs ranges from 1000 to 25000 depending on dataset size, without early stopping setting. Batch size is set to 1024. All experiments are repeated 100 times, and the mean AUC and AP (Average Precision) are reported.

**4.3.2 Link Prediction Results.** As is shown in Table 4, no matter which kind of motif is considered, the AUC and AP of GCN-MPPR is very competitive. The results further demonstrate that GCN-MPPR could propagate the information deeper and further without adding the number of layer, benefitting from the utilization of MPPR. Noticeably, the AUC and AP on *Cora* dataset surpass all baselines. This means that GCN-MPPR is still competitive when training set is limited on small-scale networks. On both *PubMed* and *Amazon\_Photo* datasets, GCN-MPPR outperforms the baselines on AUC, while performs worse than them on AP. This could be mainly attributed to the fact that MPPR tends to emphasize the global higher-order information capture, which lacks the fine-grained ranking refinement, thus hurting AP. However, even in such case the gap between GCN-MPPR and its competitors is quite narrow.

### 4.4 GCN-MPPR into other GCN Framework

GCN-MPPR shows the potential to be generalized in typical GCN tasks. As long as a part of a complicated task involves the use of any traditional GCN model to obtain representations, then by introducing the propagation optimization based on MPPR, theoretically,

**Table 4: The Results of Link Prediction via GCN-MPPR and its competitors.**

	Cora		PubMed		Amazon_Photo	
	AUC	AP	AUC	AP	AUC	AP
GCN	0.8822	0.8578	0.9582	0.9314	0.9799	0.9394
GAT	0.8722	0.8362	0.9356	0.9214	0.9725	0.9456
PPNP	0.8918	0.8657	0.9606	0.9317	0.9777	0.9351
GAE	0.8184	0.8514	0.9535	<b>0.9597</b>	0.9745	<b>0.9740</b>
VGAE	0.7490	0.7770	0.9469	0.9533	0.9696	0.9690
HDGL	0.6720	0.6862	0.8513	0.8838	0.7617	0.7706
GCN-MPPR <sub>M1</sub>	<b>0.8965</b>	<b>0.8752</b>	<b>0.9653</b>	0.9375	<b>0.9800</b>	0.9389
GCN-MPPR <sub>M2</sub>	<b>0.8973</b>	<b>0.8760</b>	<b>0.9653</b>	0.9376	<b>0.9802</b>	0.9390
GCN-MPPR <sub>M3</sub>	<b>0.8967</b>	<b>0.8751</b>	<b>0.9654</b>	0.9376	0.9798	0.9387
GCN-MPPR <sub>M4</sub>	<b>0.8921</b>	<b>0.8695</b>	<b>0.9643</b>	0.9356	0.9785	0.9383
GCN-MPPR <sub>M5</sub>	<b>0.8968</b>	<b>0.8755</b>	<b>0.9654</b>	0.9377	<b>0.9799</b>	0.9387
GCN-MPPR <sub>M6</sub>	<b>0.8974</b>	<b>0.8761</b>	<b>0.9652</b>	0.9374	<b>0.9800</b>	0.9389
GCN-MPPR <sub>M7</sub>	<b>0.8977</b>	<b>0.8757</b>	<b>0.9652</b>	0.9374	<b>0.9800</b>	0.9388
GCN-MPPR <sub>Mean</sub>	<b>0.8964</b>	<b>0.8747</b>	<b>0.9652</b>	0.9373	<b>0.9799</b>	0.9388

the performance of this GCN can be improved, thereby enhancing the overall performance of the task. To verify this, we conducted experiments on the following recently proposed framework that incorporates the GCN module. We replaced the GCN module in the overall framework with our GCN-MPPR module and verified whether the performance had improved due to the introduction of MPPR.

Consider the recent proposed Directed Graph Contrastive Representation Learning (DGCR) framework for link prediction (especially for the reconstruction for gene regulatory networks, GRNs in short). The details of DGCR can be referred to [59] and the details of the GCN-MPPR implementation on it can be referred to Appendix D. Simply speaking, the simple GCN in DGCR is replaced by GCN-MPPR to learn the representation better. The GRN reconstruction results are as shown in Table 5 (w. means with). No matter which type of motif is considered, the overall reconstruction performance increases a lot, with both AUC and AP (Average Precision) upgrading above 7% on *in silico* and 2% on *S. cerevisiae* dataset, respectively. Furthermore, it should be noted that, in such phenomenon, if the early stopping setting is removed and the training epoch is set to be extremely large, the performance of DGCR with GCN-MPPR degrades significantly, and the decline is much greater than that of DGCR. This might suggest that GCN-MPPR has some shortcomings in dealing with overfitting. The cause of this issue is still under research and might be explained by future research. However, our results are still sufficient to confirm the outstanding performance and application prospects of GCN-MPPR in many GCN tasks.

## 5 Conclusion

Graph is a ubiquitous structure that shows promise for many applications [60, 61]. MPNNs and their variants have made great successes over the past decades. However, the propagation performance of message passing neural networks are usually limited due to the fact that the propagation depth is not ‘deep enough’, leading to a series of works to solve the problem. Most existing methods tend to solve the problems via linear metrics, which are yet limited

**Table 5: GCN-MPPR into DRCRL.**

	in silico		<i>S. cerevisiae</i>	
	AUC	AP	AUC	AP
DGCRL	0.7813	0.7548	0.8194	0.7857
DGCRL w. MPPR <sub>M1</sub>	<b>0.8438</b>	<b>0.8264</b>	<b>0.8410</b>	<b>0.7986</b>
DGCRL w. MPPR <sub>M2</sub>	<b>0.8397</b>	<b>0.8207</b>	<b>0.8415</b>	<b>0.8021</b>
DGCRL w. MPPR <sub>M3</sub>	<b>0.8418</b>	<b>0.8229</b>	<b>0.8390</b>	<b>0.8000</b>
DGCRL w. MPPR <sub>M4</sub>	<b>0.8426</b>	<b>0.8214</b>	<b>0.8359</b>	<b>0.7915</b>
DGCRL w. MPPR <sub>M5</sub>	<b>0.8412</b>	<b>0.8223</b>	<b>0.8394</b>	<b>0.7969</b>
DGCRL w. MPPR <sub>M6</sub>	<b>0.8425</b>	<b>0.8267</b>	<b>0.8403</b>	<b>0.7989</b>
DGCRL w. MPPR <sub>M7</sub>	<b>0.8430</b>	<b>0.8264</b>	<b>0.8407</b>	<b>0.7961</b>
<i>Improvement</i>	$\geq 7.47\%$	$\geq 8.73\%$	$\geq 2.01\%$	$\geq 1.64\%$

to capture the higher-order structure relationships within the networks. As a result, most existing GCN models still suffer from low accuracy, limited stability and high computation cost. To overcome these challenges, MPPR is proposed as a novel variant of PageRank to record the influence of one node to another on the basis of considering higher-order motif relationships. Secondly, the MPPR is utilized to the message passing process of GCNs, thereby avoiding over-smoothing during the message passing process. The experimental results show that the proposed method outperforms almost all of the baselines on accuracy, stability and time consumption. Additionally, the proposed method can be considered as a component, that can be applied to almost all GCN tasks, with DGCRL being demonstrated in the experiments.

## References

- [1] Hanchen Wang, Ying Zhang, and Wenjie Zhang. Machine learning for graph data management and query processing. *Proc. VLDB Endow.*, 18(12):5499–5503, 2025.
- [2] Mingyang Zhou, Gang Liu, Kezhong Lu, Hao Liao, and Rui Mao. Highly-efficient minimization of network connectivity in large-scale graphs. In Guodong Long, Michale Blumestein, Yi Chang, Liane Lewin-Eytan, Zi Helen Huang, and Elad Yom-Tov, editors, *Proceedings of the ACM on Web Conference 2025, WWW 2025, Sydney, NSW, Australia, 28 April 2025- 2 May 2025*, pages 2530–2539. ACM, 2025.
- [3] Qi Chen, Zhiqiong Wang, Jiaxin Li, Jinying Tao, and Junchang Xin. TSTAi: A time-varying brain effective connectivity network construction method combining with brain active information. In *Proceedings of the Thirty-Fourth International Joint Conference on Artificial Intelligence, IJCAI 2025, Montreal, Canada, August 16-22, 2025*, pages 7347–7355. ijcai.org, 2025.
- [4] Yonghao Liu, Mengyu Li, Fausto Giunchiglia, Lan Huang, Ximing Li, Xiaoyue Feng, and Renchu Guan. Dual-level mixup for graph few-shot learning with fewer tasks. In Guodong Long, Michale Blumestein, Yi Chang, Liane Lewin-Eytan, Zi Helen Huang, and Elad Yom-Tov, editors, *Proceedings of the ACM on Web Conference 2025, WWW 2025, Sydney, NSW, Australia, 28 April 2025- 2 May 2025*, pages 2646–2656. ACM, 2025.
- [5] Chengjie Zhao, Jun Wang, Qihang Peng, Wei Huang, Xiaonan Chen, Zexue Zhao, and Tho Le-Ngoc. Deep learning based transceiver design for additive non-gaussian impulsive noise channels. *IEEE Transactions on Cognitive Communications and Networking*, pages 1–1, 2025.
- [6] Badil Ghazi, Ravi Kumar, and Pasin Manurangsi. Privacy in web advertising: Analytics and modeling. In Tat-Seng Chua, Chong-Wah Ngo, Roy Ka-Wei Lee, Ravi Kumar, and Hady W. Lauw, editors, *Companion Proceedings of the ACM on Web Conference 2024, WWW 2024, Singapore, Singapore, May 13-17, 2024*, pages 1288–1289. ACM, 2024.
- [7] Yurui Lai, Xiaoyang Lin, Renchi Yang, and Hongtao Wang. Efficient topology-aware data augmentation for high-degree graph neural networks. In Ricardo Baeza-Yates and Francesco Bonchi, editors, *Proceedings of the 30th ACM SIGKDD Conference on Knowledge Discovery and Data Mining, KDD 2024, Barcelona, Spain, August 25-29, 2024*, pages 1463–1473. ACM, 2024.
- [8] Yang Tang, Zhongming Xie, Yuhai Fan, Kaiyang Zhong, and Muhammet Deveci. Inferring anti-viral drugs using nonnegative matrix factorization with self-paced learning and hypergraph regularization. *Expert Syst. Appl.*, 296:129104, 2026.
- [9] Wang Zhou, Zhiqian Liu, Amin Ul Haq, Yuehui Li, and Zoe L. Jiang. Differentially private matrix factorization with sub-linear convergence rate for personalized recommendation. *Inf. Fusion*, 126:103621, 2026.
- [10] Yang Yi, Xuequan Lu, Shang Gao, Antonio Robles-Kelly, and Yuejie Zhang. Graph classification via discriminative edge feature learning. *Pattern Recognit.*, 143:10799, 2023.
- [11] Jingwei Guo, Kaizhu Huang, Xinpeng Yi, and Rui Zhang. Graph neural networks with diverse spectral filtering. In *WWW*, pages 306–316. ACM, 2023.
- [12] Mingguo He, Zhewei Wei, Shikun Feng, Zhengjie Huang, Weibin Li, Yu Sun, and Dianhai Yu. Spectral heterogeneous graph convolutions via positive noncommutative polynomials. In *WWW*, pages 685–696. ACM, 2024.
- [13] Tiantian He, Yang Liu, Yew-Soon Ong, Xiaohu Wu, and Xin Luo. Polarized message-passing in graph neural networks. *Artif. Intell.*, 331:104129, 2024.
- [14] Zhifei Li, Lifan Chen, Yue Jian, Han Wang, Yue Zhao, Miao Zhang, Kui Xiao, Yan Zhang, Honglian Deng, and Xiaoju Hou. Aggregation or separation? adaptive embedding message passing for knowledge graph completion. *Information Sciences*, 691:121639, 2025.
- [15] Mounir Ghogho. Revisiting neighborhood aggregation in graph neural networks for node classification using statistical signal processing. In *ICASSP 2025-2025 IEEE International Conference on Acoustics, Speech and Signal Processing (ICASSP)*, pages 1–5. IEEE, 2025.
- [16] Di Jin, Rui Wang, Meng Ge, Dongxiao He, Xiang Li, Wei Lin, and Weixiong Zhang. RAW-GNN: random walk aggregation based graph neural network. In Luc De Raedt, editor, *Proceedings of the Thirty-First International Joint Conference on Artificial Intelligence, IJCAI 2022, Vienna, Austria, 23-29 July 2022*, pages 2108–2114. ijcai.org, 2022.
- [17] Yizhou Chen, Anxiang Zeng, Qingtao Yu, Kerui Zhang, Cao Yuanpeng, Kangle Wu, Guangda Huzhang, Han Yu, and Zhiming Zhou. Recurrent temporal revision graph networks. *Advances in Neural Information Processing Systems*, 36:69348–69360, 2023.
- [18] Shu Li, Nayyar A Zaidi, Meijie Du, Zhou Zhou, Hongfei Zhang, and Gang Li. Property graph representation learning for node classification. *Knowledge and Information Systems*, 66(1):237–265, 2024.
- [19] Jongmin Park, Seunghoon Han, Soohwan Jeong, and Sungsu Lim. Hyperbolic heterogeneous graph attention networks. In Tat-Seng Chua, Chong-Wah Ngo, Roy Ka-Wei Lee, Ravi Kumar, and Hady W. Lauw, editors, *Companion Proceedings of the ACM on Web Conference 2024, WWW 2024, Singapore, Singapore, May 13-17, 2024*, pages 561–564. ACM, 2024.
- [20] Huiyuan Chen, Chin-Chia Michael Yeh, Fei Wang, and Hao Yang. Graph neural transport networks with non-local attentions for recommender systems. In

Frédérique Laforest, Raphaël Troncy, Elena Simperl, Deepak Agarwal, Aristides Gionis, Ivan Herman, and Lionel Médini, editors, *WWW '22: The ACM Web Conference 2022, Virtual Event, Lyon, France, April 25 - 29, 2022*, pages 1955–1964. ACM, 2022.

[21] Dong Zhang, Wenlong Feng, Zonghang Wu, Guanyu Li, and Bo Ning. CDRGN-SDE: cross-dimensional recurrent graph network with neural stochastic differential equation for temporal knowledge graph embedding. *Expert Syst. Appl.*, 247:123295, 2024.

[22] Soheila Molaei, Nima Ghanbari Bousejin, Ghadeer O. Ghosheh, Anshul Thakur, Vinod Kumar Chauhan, Tingting Zhu, and David A. Clifton. Cliquefluxnet: Unveiling EHR insights with stochastic edge fluxing and maximal clique utilisation using graph neural networks. *J. Heal. Informatics Res.*, 8(3):555–575, 2024.

[23] Johannes Klicpera, Aleksandar Bojchevski, and Stephan Günnemann. Predict then propagate: Graph neural networks meet personalized pagerank. In *7th International Conference on Learning Representations, ICLR 2019, New Orleans, LA, USA, May 6-9, 2019*. OpenReview.net, 2019.

[24] Aleksandar Bojchevski, Johannes Klicpera, Bryan Perozzi, Amol Kapoor, Martin Blais, Benedek Rózemberczki, Michal Lukasik, and Stephan Günnemann. Scaling graph neural networks with approximate pagerank. In Rajesh Gupta, Yan Liu, Jiliang Tang, and B. Aditya Prakash, editors, *KDD '20: The 26th ACM SIGKDD Conference on Knowledge Discovery and Data Mining, Virtual Event, CA, USA, August 23-27, 2020*, pages 2464–2473. ACM, 2020.

[25] Yiming Li, Yanyan Shen, Lei Chen, and Mingxuan Yuan. Zebra: When temporal graph neural networks meet temporal personalized pagerank. *Proc. VLDB Endow.*, 16(6):1332–1345, 2023.

[26] MoonJeong Park, Sunghyun Choi, Jaeseung Heo, Eunhyeok Park, and Dongwoo Kim. The oversmoothing fallacy: A misguided narrative in GNN research. *CoRR*, abs/2506.04653, 2025.

[27] Weichen Zhao, Chenguang Wang, Xinyan Wang, Congying Han, Tiande Guo, and Tianshu Yu. Understanding oversmoothing in diffusion-based gnns from the perspective of operator semigroup theory. In *Proceedings of the 31st ACM SIGKDD Conference on Knowledge Discovery and Data Mining V.1, KDD '25*, page 2043–2054, New York, NY, USA, 2025. Association for Computing Machinery.

[28] Nicolas Keriven. Backward oversmoothing: why is it hard to train deep graph neural networks? *CoRR*, abs/2505.16736, 2025.

[29] Zhijian Zhuo, Yifei Wang, Jinwen Ma, and Yisen Wang. Graph neural networks (with proper weights) can escape oversmoothing. In Vu Nguyen and Hsuan-Tien Lin, editors, *Proceedings of the 16th Asian Conference on Machine Learning*, volume 260 of *Proceedings of Machine Learning Research*, pages 17–32. PMLR, 05–08 Dec 2025.

[30] Dimitrios Kelesis, Dimitris Fotakis, and Georgios Paliouras. Reducing oversmoothing through informed weight initialization in graph neural networks. *Appl. Intell.*, 55(7):632, 2025.

[31] Thomas N. Kipf and Max Welling. Variational graph auto-encoders. *CoRR*, abs/1611.07308, 2016.

[32] R. Milo, S. Shen-Orr, S. Itzkovitz, N. Kashtan, D. Chklovskii, and U. Alon. Network motifs: Simple building blocks of complex networks. *Science*, 298(5594):824–827, 2002.

[33] Nesreen K. Ahmed, Jennifer Neville, Ryan A. Rossi, and Nick G. Duffield. Efficient graphlet counting for large networks. In Charu C. Aggarwal, Zhi-Hua Zhou, Alexander Tuzhilin, Hui Xiong, and Xindong Wu, editors, *2015 IEEE International Conference on Data Mining, ICDM 2015, Atlantic City, NJ, USA, November 14-17, 2015*, pages 1–10. IEEE Computer Society, 2015.

[34] Madhav Jha, C. Seshadhri, and Ali Pinar. Path sampling: A fast and provable method for estimating 4-vertex subgraph counts. In Aldo Gangemi, Stefano Leonardi, and Alessandro Panconesi, editors, *Proceedings of the 24th International Conference on World Wide Web, WWW 2015, Florence, Italy, May 18-22, 2015*, pages 495–505. ACM, 2015.

[35] Radu Curticapean and Daniel Neuen. Counting small induced subgraphs: Hardness via fourier analysis. In Yossi Azar and Debmalya Panigrahi, editors, *Proceedings of the 2025 Annual ACM-SIAM Symposium on Discrete Algorithms, SODA 2025, New Orleans, LA, USA, January 12-15, 2025*, pages 3677–3695. SIAM, 2025.

[36] Rong-Hua Li, Xiaowei Ye, Fusheng Jin, Yu-Ping Wang, Ye Yuan, and Guoren Wang. Counting cohesive subgraphs with hereditary properties. In Guodong Long, Michale Blumestein, Yi Chang, Liane Lewin-Eytan, Zi Helen Huang, and Elad Yom-Tov, editors, *Proceedings of the ACM on Web Conference 2025, WWW 2025, Sydney, NSW, Australia, 28 April 2025- 2 May 2025*, pages 3874–3884. ACM, 2025.

[37] Xin Zheng, Guiling Wang, Guiyue Xu, Jianye Yang, Boyang Han, and Jian Yu. A llm-driven and motif-informed linearizing graph transformer for web API recommendation. *Appl. Soft Comput.*, 169:112547, 2025.

[38] Rong-Hua Li, Xiaowei Ye, Fusheng Jin, Yu-Ping Wang, Ye Yuan, and Guoren Wang. Counting cohesive subgraphs with hereditary properties. In Guodong Long, Michale Blumestein, Yi Chang, Liane Lewin-Eytan, Zi Helen Huang, and Elad Yom-Tov, editors, *Proceedings of the ACM on Web Conference 2025, WWW 2025, Sydney, NSW, Australia, 28 April 2025- 2 May 2025*, pages 3874–3884. ACM, 2025.

[39] Huan Zhao, Xiaogang Xu, Yangqin Song, Dik Lun Lee, Zhao Chen, and Han Gao. Ranking users in social networks with motif-based pagerank. *IEEE Transactions on Knowledge and Data Engineering*, 33(5):2179–2192, 2021.

[40] Xunlian Wu, Jingqi Hu, Yining Quan, Qiguang Miao, and Peng Gang Sun. Motif-based contrastive graph clustering with clustering-oriented prompt. *Information Processing & Management*, 62(5):104208, 2025.

[41] Lawrence Page, Sergey Brin, Rajeev Motwani, and Terry Winograd. The pagerank citation ranking: Bringing order to the web. *Stanford Digital Libraries Working Paper*, 1998.

[42] ZHAO Hai, MIAO Jiu, nan, LIU Xiao, and YU Xue, long. Identification of key nodes of acupoint-disease network based on motif pagerank algorithm. *Journal of Northeastern University (Natural Science)*, 45(5):628–635, 2024.

[43] Cataldo Musto, Pasquale Lops, Marco de Gemmis, and Giovanni Semeraro. Context-aware graph-based recommendations exploiting personalized pagerank. *Knowl. Based Syst.*, 216:106806, 2021.

[44] Jiahui Hu, Jie Xu, Jiakun Chen, LiQiang Qiao, Jilu Wang, Feiran Huang, and Chaozhou Li. Detaching range from depth: Personalized recommendation meets personalized pagerank. In Rafik Hadfi, Patricia Anthony, Alok Sharma, Takayuki Ito, and Quan Bai, editors, *PRICAI 2024: Trends in Artificial Intelligence - 21st Pacific Rim International Conference on Artificial Intelligence, PRICAI 2024, Kyoto, Japan, November 18-24, 2024, Proceedings, Part I*, volume 15281 of *Lecture Notes in Computer Science*, pages 454–466. Springer, 2024.

[45] Ke Ma, Jiawei Li, Mengyuan Zhao, Ibrahim Zamit, Bin Lin, Fei Guo, and Jijun Tang. PPRTGI: A personalized pagerank graph neural network for tf-target gene interaction detection. *IEEE ACM Trans. Comput. Biol. Bioinform.*, 21(3):480–491, 2024.

[46] Monica Bianchini, Marco Gori, and Franco Scarselli. Inside pagerank. *ACM Trans. Internet Techn.*, 5(1):92–128, 2005.

[47] Austin R. Benson, David F. Gleich, and Jure Leskovec. Higher-order organization of complex networks. *Science*, 353(6295):163–166, 2016.

[48] Zhongmin Pei, Boren Hu, Zhangkai Luo, and Jie Ding. Analysis of node importance of satellite network based on triangular motif. In *Proceedings of the 2023 International Conference on Communication Network and Machine Learning, CNML 2023, Zhengzhou, China, October 27-28, 2023*, pages 6–12. ACM, 2023.

[49] Hyeonseong Jeon, Suh-Ryung Kim, Doug Nam, and Yun Joo Yoo. Analysis of triangular motifs in protein interaction networks and their implications to protein ages and cancer genes. *Int. J. Data Min. Bioinform.*, 19(4):340–365, 2017.

[50] Prithviraj Sen, Galileo Namata, Mustafa Bilgic, Lise Getoor, Brian Gallagher, and Tina Eliassi-Rad. Collective classification in network data. *AI Mag.*, 29(3):93–106, 2008.

[51] Galileo Namata, Ben London, and Bert Huang Namatag. Query-driven active surveying for collective classification. 2012.

[52] Oleksandr Shchur, Maximilian Mumme, Aleksandar Bojchevski, and Stephan Günnemann. Pitfalls of graph neural network evaluation. *CoRR*, abs/1811.05868, 2018.

[53] Thomas N. Kipf and Max Welling. Semi-supervised classification with graph convolutional networks. In *5th International Conference on Learning Representations, ICLR 2017, Toulon, France, April 24-26, 2017, Conference Track Proceedings*. OpenReview.net, 2017.

[54] Petar Velickovic, Guillem Cucurull, Arantxa Casanova, Adriana Romero, Pietro Liò, and Yoshua Bengio. Graph attention networks. In *6th International Conference on Learning Representations, ICLR 2018, Vancouver, BC, Canada, April 30 - May 3, 2018, Conference Track Proceedings*. OpenReview.net, 2018.

[55] Keyulu Xu, Weihua Hu, Jure Leskovec, and Stefanie Jegelka. How powerful are graph neural networks? In *7th International Conference on Learning Representations, ICLR 2019, New Orleans, LA, USA, May 6-9, 2019*. OpenReview.net, 2019.

[56] Fei Yang, Huyin Zhang, Shiming Tao, and Xiying Fan. Simple hierarchical pagerank graph neural networks. *J. Supercomput.*, 80(4):5509–5539, 2024.

[57] Abhishek Dalvi and Vasanth G. Honavar. Hyperdimensional representation learning for node classification and link prediction. In Wolfgang Nejdl, Sören Auer, Meeyoung Cha, Marie-Francine Moens, and Marc Najork, editors, *Proceedings of the Eighteenth ACM International Conference on Web Search and Data Mining, WSDM 2025, Hannover, Germany, March 10-14, 2025*, pages 88–97. ACM, 2025.

[58] Haoyu Liu and Siqiang Luo. BIRD: efficient approximation of bidirectional hidden personalized pagerank. *Proc. VLDB Endow.*, 17(9):2255–2268, 2024.

[59] Kaifu Long, Luxuan Qu, Weiyiqi Wang, Zhiqiong Wang, Mingcan Wang, and Junchang Xin. Inferring gene regulatory networks via directed graph contrastive representation learning. *Knowledge-Based Systems*, 316:113324, 2025.

[60] Xiaoyang Lin, Runhao Jiang, and Renchi Yang. Effective clustering for large multi-relational graphs. *Proc. ACM Manag. Data*, 3(6):1–28, 2025.

[61] Haoran Zheng, Jieming Shi, and Renchi Yang. Grasp: Simple yet effective graph similarity predictions. In Toby Walsh, Julie Shah, and Zico Kolter, editors, *AAAI-25, Sponsored by the Association for the Advancement of Artificial Intelligence, February 25 - March 4, 2025, Philadelphia, PA, USA*, pages 22884–22892. AAAI Press, 2025.

## Appendix

### A The Motif-Based Adjacency Matrices Calculation of the Seven Considered Motifs.

In this section, the motif-based adjacency matrices calculation process of seven kinds of motifs are represented. For a graph  $G$ , whose adjacency matrix is marked as  $A$ , let  $U$  ( $B$ , respectively) be the adjacency matrix of the unidirectional (bidirectional, respectively) links of  $G$ . Then the motif-based adjacency matrices of graph  $G$  with respect to  $M_1$  to  $M_7$  is calculated as Table 6.

**Table 6: The Motif-Based Adjacency Matrices Calculation.**

Motif	Intermediate Matrix	$A_{M_i}$
$M_1$	$\zeta = (U \cdot U) \odot U^T$	$\zeta + \zeta^T$
$M_2$	$\zeta = (B \cdot U) \odot U^T + (U \cdot B) \odot U^T + (U \cdot U) \odot B$	$\zeta + \zeta^T$
$M_3$	$\zeta = (B \cdot B) \odot U + (B \cdot U) \odot B + (U \cdot B) \odot B$	$\zeta + \zeta^T$
$M_4$	$\zeta = (B \cdot B) \odot B$	$\zeta$
$M_5$	$\zeta = (U \cdot U) \odot U + (U \cdot U^T) \odot U + (U^T \cdot U) \odot U$	$\zeta + \zeta^T$
$M_6$	$\zeta = (U \cdot B) \odot U + (B \cdot U^T) \odot U^T + (U^T \cdot U) \odot B$	$\zeta$
$M_7$	$\zeta = (U^T \cdot B) \odot U^T + (B \cdot U) \odot U + (U \cdot U^T) \odot B$	$\zeta$

The table is grabbed from [39, 47].  $\odot$  denotes the Hadamard (entry-wise) product.

### B The Details of the Datasets.

Cora [50] and PubMed [51] are famous and widely applied citation graphs, where nodes represent papers and the edges represent citations between them. Amazon Computers and Amazon Photo [52] are both segments of the Amazon co-purchase graph, where nodes represent goods, edges indicate that two goods are frequently bought together, node features are bag-of-words encoded product reviews, and class labels are given by the product category. The statistics information of these networks are as shown in Table 7.

**Table 7: The Statistics of Datasets.**

	Classes	Features	Nodes	Edges
Cora	7	1433	2845	5069
PubMed	3	500	19717	44324
Amazon Computers	10	767	13381	245778
Amazon Photo	8	745	7487	119043

### C Analysis of the stability of GCN-MPPR

In order to further verify the stability of GCN-MPPR, the classification accuracy of each run on multiple networks is collected and presented in Figure 4. In each box figures, the box on the far left is the best performer of each network, while the other 7 boxes represent the results of GCN-MPPR with  $M_1$  to  $M_7$ . Although in some cases the top limit of accuracy achieved by the best baselines is higher, in almost all cases the lower limit of GCN-MPPR has been significantly improved. Meanwhile, the box of GCN-MPPR is comparatively shorter. As a result, together with Table 1, it is confirmed that GCN-MPPR not only improves the accuracy but also enhances the stability.

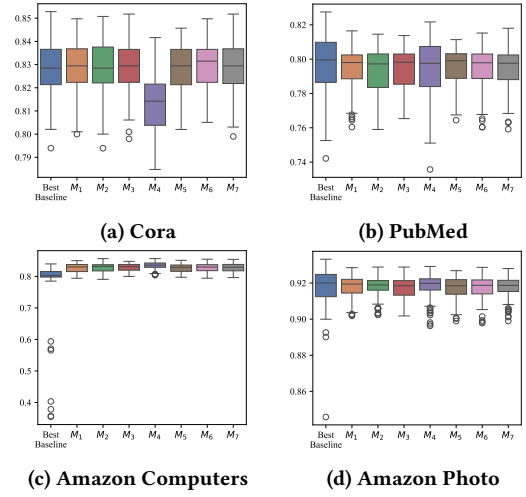


**Figure 4: The Box Figures of a Hundred Runs on Various Datasets.**

### D The Details of the GCN-MPPR Implementation on DGCRL.

In DGCRL, the model of GCN is applied. In order to implement GCN-MPPR upon DGCRL, we multiply the calculated MPPR to the output of the encoder on DGCRL, thereby making the information of each node transfer deeper and further without adding layers. And all of other technical details are hold on still without any modification. As for the experiment, the settings are list in Table 8.

**Table 8: Implementation Parameter Details of GCN-MPPR on DGCRL.**

Parameter	Value	Parameter	Value
Train/Val/Test	2:4:4	Hidden Dimansion of Layer	128
Training Epochs	500	Out Dimansion of Encoder	16
Learning Rate	0.01	Hidden Dimansion of Decoder	128
$p_{r,1}, p_{r,2}, p_{m,1}, p_{m,2}$	0.1	Negative Sampling Ratio	1.0